

Grating pitch comparison measurement based on Cr atomic transition frequency and Si lattice constant

Jingtong Feng(冯婧桐), Rao Xu(徐娆), Ziruo Wu(吴子若), Lihua Lei(雷李华), Yingfan Xiong(熊英凡), Zhaohui Tang(唐朝辉), Guangxu Xiao(肖光旭), Yuying Xie(解钰莹), Dongbai Xue(薛栋柏), Xiao Deng(邓晓), Xinbin Cheng(程鑫彬), and Tongbao Li(李同保)

Citation: Chin. Phys. B, 2025, 34 (**2**): 020601. DOI: 10.1088/1674-1056/ad9e9a
Journal homepage: http://cpb.iphy.ac.cn; http://iopscience.iop.org/cpb

What follows is a list of articles you may be interested in

A real-time performance improvement method for composite time scale

Fangmin Wang(王芳敏), Wenlin Li(李汶林), Hongfei Dai(戴鸿飞), Chunyi Li(李春怡), Jianhua Zhou(周建华), Shenhui Xue(薛申辉), and Bo Wang(王波)

Chin. Phys. B, 2024, 33 (**9**): 090601. DOI: 10.1088/1674-1056/ad6131

Nonlinear time-reversal interferometry with arbitrary quadratic collective-spin interaction

Zhiyao Hu(胡知遥), Qixian Li(李其贤), Xuanchen Zhang(张轩晨), He-Bin Zhang(张贺宾), Long-Gang Huang(黄龙刚), and Yong-Chun Liu(刘永椿)

Chin. Phys. B, 2024, 33 (**8**): 080601. DOI: 10.1088/1674-1056/ad4ff7

Measuring small longitudinal phase shifts via weak measurement amplification

Kai Xu(徐凯), Xiao-Min Hu(胡晓敏), Meng-Jun Hu(胡孟军), Ning-Ning Wang(王宁宁), Chao Zhang(张超), Yun-Feng Huang(黄运锋), Bi-Heng Liu(柳必恒), Chuan-Feng Li(李传锋), Guang-Can Guo(郭光灿), and Yong-Sheng Zhang(张永生)

Chin. Phys. B, 2024, 33 (**3**): 030602. DOI: 10.1088/1674-1056/ad1c5a

Feedback control and quantum error correction assisted quantum multi-parameter estimation

Hai-Yuan Hong(洪海源), Xiu-Juan Lu(鲁秀娟), and Sen Kuang(匡森)

Chin. Phys. B, 2023, 32 (**4**): 040603. DOI: 10.1088/1674-1056/ac8721

Optimization of laser focused atomic deposition by channeling

Jie Chen(陈杰), Jie Liu(刘杰), Li Zhu(朱立), Xiao Deng(邓晓), Xinbin Cheng(陈鑫彬), Tongbao Li(李同保)

Chin. Phys. B, 2020, 29 (**2**): 020601. DOI: 10.1088/1674-1056/ab631c

---

INSTRUMENTATION AND MEASUREMENT

Grating pitch comparison measurement based on Cr atomic transition frequency and Si lattice constant

Jingtong Feng(冯婧桐)[1,2,3,4,5,6], Rao Xu(徐娆)[1,2,3,4,5,6], Ziruo Wu(吴子若)[7], Lihua Lei(雷李华)[8], Yingfan Xiong(熊英凡)[1,2,3,4,5,6], Zhaohui Tang(唐朝辉)[1,2,3,4,5,6], Guangxu Xiao(肖光旭)[1,2,3,4,5,6], Yuying Xie(解钰莹)[1,2,3,4,5,6,†], Dongbai Xue(薛栋柏)[1,2,3,4,5,6], Xiao Deng(邓晓)[1,2,3,4,5,6], Xinbin Cheng(程鑫彬)[1,2,3,4,5,6], and Tongbao Li(李同保)[1,2,3,4,5,6]

[1] *National Metrology and Testing Center for Integrated Circuit Measurement and Inspection Equipment Industry (Shanghai), Tongji University, Shanghai* 200092, *China*

[2] *Institute of Precision Optical Engineering, Tongji University, Shanghai* 200092, *China*

[3] *MOE Key Laboratory of Advanced Micro-Structured Materials, Tongji University, Shanghai* 200092, *China*

[4] *Shanghai Frontiers Science Center of Digital Optics, Tongji University, Shanghai* 200092, *China*

[5] *Shanghai Professional Technical Service Platform for Full-Spectrum and High-Performance Optical Thin Film Devices and Applications, Tongji University, Shanghai* 200092, *China*

[6] *School of Physics Science and Engineering, Tongji University, Shanghai* 200092, *China*

[7] *Shanghai Metric Optics Technology Co., Ltd., Shanghai* 201108, *China*

[8] *Shanghai Institute of Measurement and Testing Technology, Shanghai* 201203, *China*

(Received 29 September 2024; revised manuscript received 12 November 2024; accepted manuscript online 13 December 2024)

Traceability is the fundamental premise of all metrological activities. The establishment of a traceability chain characterized by a shortened structure, while simultaneously enabling on-site traceability, represents a key trend in the advancement of metrology. This study explores the periodic accuracy and overall uniformity of self-traceable gratings, employing multilayer film gratings with a nominal period of 25.00 nm as the medium. We present a comparative analysis of measurement capabilities in a self-traceable grating calibration system characterized by a 'top-down' calibration approach and a Si lattice constant calibration system characterized by a 'bottom-up' calibration approach. The results indicate that the values obtained for the multilayer film grating periods, calibrated using the self-traceable grating system, are 24.40 nm with a standard deviation of 0.11 nm. By comparing with the values derived from the Si lattice constant, which yield 24.34 nm with a standard deviation of 0.14 nm, the validity and feasibility of the self-traceable calibration system are confirmed. This system extends and complements existing metrological frameworks, offering a precise pathway for traceability in precision engineering and nanotechnology research.

Keywords: nanometrology, self-traceable standard material, Si lattice constant

PACS: 06.20.–f, 06.20.fb, 81.07.–b

DOI: 10.1088/1674-1056/ad9e9a **CSTR:** 32038.14.CPB.ad9e9a

1. Introduction

In the field of nanometrology, the continuous miniaturization of manufacturing processes presents increasing challenges for measurements at the nanoscale. Ensuring the traceability and accuracy of various critical dimensions (CD), feature shapes, and profile characterization results is particularly crucial.[1] The precise measurement and characterization of these parameters are key steps in ensuring product quality, optimizing process parameters, and calibrating measurement equipment, holding significant importance in industries such as manufacturing, microelectronics, and integrated circuits. For instance, in integrated circuit chip manufacturing, as the logical structure size of chips reaches below 3 nm, the chip structures have expanded from two-dimensional to three-dimensional. This necessitates the use of a combination of optical, probe, electronic, and x-ray measurement devices for accurate characterization.[2] Different fusion measurement devices require various calibration methods, highlighting the need to establish distinct nanometrological systems to meet the demands of integrated measurement.

In the existing nanometrology systems, there are primarily two methods for achieving traceable measurements: one is the 'top-down' traceability chain based on laser wavelength, and the other is the 'bottom-up' traceability chain based on the Si lattice constant. The I_2-stabilized 633 nm He–Ne laser radiation serves as a typical representative of the 'top-down' length traceability chain, where the value transfer process is as follows: International System of Units 'metre' → I_2-stabilized 633 nm He–Ne laser interferometer → metrological testing instruments → standard materials → user instruments. This traceability chain requires calibration through three steps,

[†]Corresponding author. E-mail: 23310117@tongji.edu.cn

© 2025 Chinese Physical Society and IOP Publishing Ltd. All rights, including for text and data mining, AI training, and similar technologies, are reserved.

leading to issues such as value accumulation due to the length of the traceability chain and low calibration efficiency, resulting in continuously decreasing calibration accuracy[3] (Fig. 1). The second method utilizes the Si lattice constant as the reference for a 'bottom-up' traceability chain. In 2018, the 26th International Conference on Weights and Measures recommended using the Si lattice spacing ($d_{220} = 192.0155714 \times 10^{-12}$ m) as an auxiliary means for the definition of the meter in nanometric geometric applications.[4] This established a 'bottom-up' value transfer method that employs the Si lattice spacing as an internal ruler to determine the dimensions of nanostructures. In static applications, to obtain atomically resolved measurement images, transmission electron microscopy (TEM) is generally employed, which is considered a destructive measurement. Meanwhile, in dynamic applications, the displacement measurement range of x-ray lattice interferometers is typically around 10 μm, making the expansion of the measurement range a key area of research.

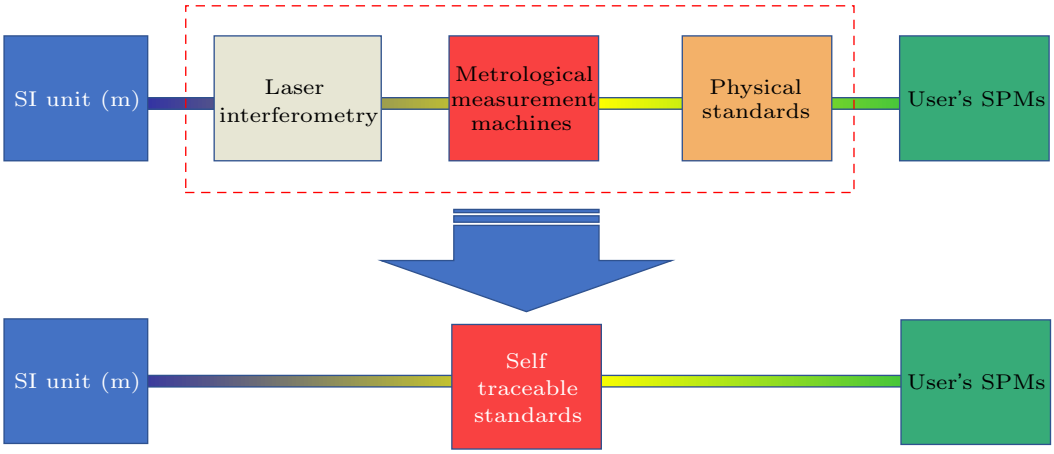


Fig. 1. Comparison of the traditional traceability chain based on wavelength (upper) and the self-traceable shortened traceability chain (lower).[3]

To meet the metrological testing requirements in the field of micro-displacement measurements for advanced nanofabrication, the team led by Academician Tongbao Li from Tongji University proposed a shortened nanometrology system based on Cr self-traceable gratings.[3] The core of this system lies in the application of atomic lithography technology to materialize the physical wavelength standard corresponding to the Cr atomic transition frequency of $^7S_3 \rightarrow {}^7P_4$ into self-traceable gratings, which can be directly used for calibrating measurement instruments. A value comparison with the metrological atomic force microscope (AFM) from the Physikalisch-Technische Bundesanstalt (PTB) confirmed the feasibility of the traceability chain based on Cr self-traceable gratings. This self-traceable calibration system not only shortens the traceability chain and enhances calibration efficiency but also serves as a beneficial complement to traditional 'top-down' calibration systems based on laser wavelength standards.[3]

However, the comparison between different traceability chains is crucial for verifying the accuracy of the value transfer system. The research team led by Gaoliang Dai conducted comparative measurements of Si structure linewidths by contrasting the 'top-down' and 'bottom-up' traceability systems.[5] The measurement results demonstrate that each method possesses distinct advantages and limitations, with the 'bottom-up' approach demonstrating higher measurement resolution and accuracy. The comparative measurement of the metrological means from both traceability methods is beneficial for enhancing overall calibration capability. Based on this, we recognize the importance of conducting comparisons between different traceability chains. Currently, the self-traceable calibration system has only undergone value comparisons with the 'top-down' calibration system.

To conduct a comparative study on the accuracy between Cr self-traceable gratings and Si lattice constants, it is essential to select appropriate measurement instruments and comparison measurement substrates. In terms of measurement instruments, AFM, with its capability to image at the nanoscale and even atomic level, has become a key tool for obtaining critical data such as surface roughness and morphology. However, it is well known that due to the inherent characteristics of piezoelectric ceramics, there is a nonlinear relationship between the actual displacement of the scanner and the applied voltage during the measurement process, which can introduce measurement errors of 5% to 10%.[6] Thus, selecting AFM as the comparative measurement instrument is an effective means to validate the cross-scale calibration accuracy of self-traceable gratings. Regarding the comparison measurement substrates, on the one hand, atomic-level images must be obtained for the substrates, necessitating that the grating period should generally not exceed 50 nm. On the other hand, since AFM and TEM cannot be positioned on the same area, the structural consistency and uniformity within the comparison substrate itself are critical; otherwise, the results may only reflect structural deviations within the sample. The core

of multilayer film deposition technology is to translate film thickness into linewidth structures, providing exceptional uniformity while enabling the fabrication of sub-50 nm grating structures, thus offering advantages in uniformity as a comparison substrate. Additionally, the Si substrate of the Si/SiO_2 multilayer film grating technology provides atomic-level interplanar spacing information for the calibration of grating period or linewidth,[7] thereby meeting the stringent requirements for both Si lattice constant and self-traceable grating comparisons.

Inspired by the above factors, this study proposes to utilize multilayer film gratings as the comparison substrate and employ AFM and TEM as measurement tools to conduct a comparative study on the metrological calibration accuracy between self-traceable gratings based on Cr atomic transition frequency and Si lattice constants. This research leverages the periodic accuracy and consistency of self-traceable gratings to directly calibrate the AFM, ensuring the traceability and accuracy of its measurement results. By customizing the linewidth measurement of the TEM based on the Si lattice constant, the traceability and accuracy of the TEM measurements can be guaranteed. Additionally, the excellent uniformity of multilayer film gratings ensures structural consistency in the comparative measurements. The research aims to verify the accuracy and consistency levels of different value transfer methods through comparative studies. This study holds significant importance for the integrated circuit field regarding the hybird measurement and metrology of gratings and linewidths.

2. Principal, fabrication and measurements

2.1. Manufacturing principle of self-traceable gratings

Using Cr as a case study, the self-traceable grating technology materializes the physical standard wavelength by precisely locking onto the specific transition frequency ($^7S_3$–$^7P_4$) of Cr atoms, thereby establishing traceability of the grating pitch to the wavelength value corresponding to this transition frequency.[8] The manufacturing process entails evaporating Cr in a vacuum environment at approximately 1600 °C to generate a Cr atomic beam. A laser, intentionally detuned relative to the transition frequency, is employed to cool the lateral velocity of the selected Cr atomic beam through the Doppler cooling principle. The collimated Cr atoms are subsequently converged within the laser standing wave field, where deposition occurs at the antinode or node positions according to the wavelength detuning, resulting in the formation of a periodic one-dimensional grating structure characterized by high accuracy and reliability, as illustrated in Fig. 2. Two laser beams are stabilized near the $^7S_3 \rightarrow {}^7P_4$ transition frequency of Cr atoms, leading to a grating pitch that is half the wavelength of the standing wave field, which is traceable to the transition frequency of the Cr atom. Consequently, the Cr grating pitch exhibits self-traceable properties. The one-dimensional self-traceable grating produced via this method demonstrates exceptional accuracy and consistency, with measurements on the order of 0.001 nm.[3,9]

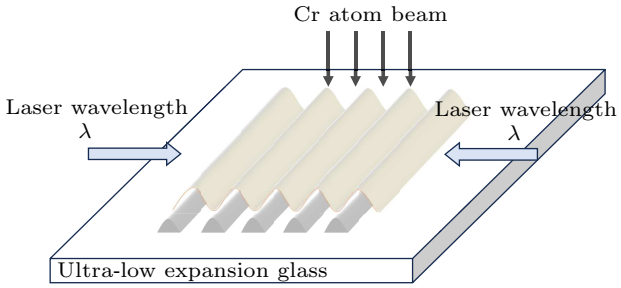


Fig. 2. Principle of the Cr self-traceable grating.[3,9]

2.2. Manufacturing of multilayer film gratings

The manufacturing process of multilayer film gratings is a technique that translates the thickness values of deposited film layers into linewidth and grating pitch measurements.[10] The preparation workflow is depicted in Fig. 3. Utilizing ion beam sputtering technology, we sequentially deposit alternating layers of 15 nm Si and 10 nm SiO_2 to construct the multilayer film structure. In this configuration, the 15 nm Si layer is designated as the linewidth, while the 10 nm SiO_2 layer acts as a spacer, with the entire structure repeated for 60 cycles. This arrangement ensures stability and exceptional uniformity among the film layers across a broad range. Following this, two samples with identical deposited film layers undergo processes of bonding, cutting, grinding, and polishing. Wet etching is then performed using an HF solution to produce standard samples, which are subsequently mounted on a substrate for further application.

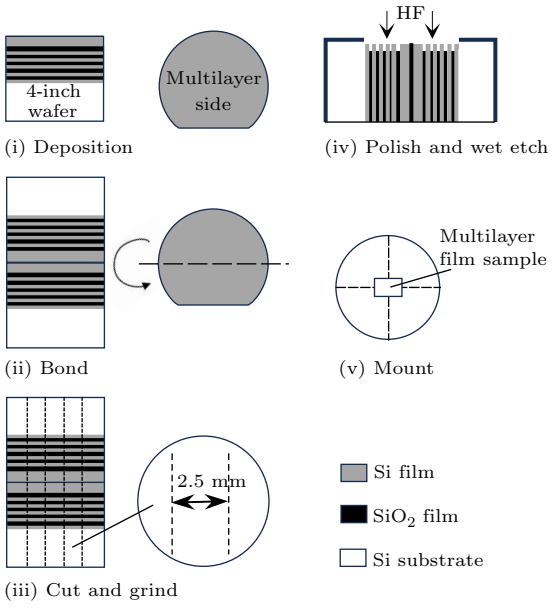


Fig. 3. Fabrication process of the multilayer film grating.[10]

2.3. Measurement methods for grating pitch

For grating images obtained via AFM, the gravity center method is commonly employed to calculate the grating period.[11,12] This method centers on determining a threshold line between the top and bottom lines of the grating structure based on a preset percentage $p\%$, and subsequently calculating the centroid of the upper structure above this threshold line to accurately ascertain the average grating pitch and positional deviation, as illustrated in Fig. 4. The specific process is as follows: (i) Removal of ripple artifacts: The grating profiles obtained from AFM measurements often exhibit undesirable ripple artifacts coupled with the actual profiles, leading to erroneous identification of structural boundaries and impacting measurement accuracy. Therefore, this study first employs a phase-corrected low-pass filter to process the profile data, effectively recognizing and filtering out ripple artifacts. (ii) Profile line interpolation: Given that the grating profile is sampled as discrete data at a certain pixel density, the limitation in pixel quantity makes it challenging to accurately determine the boundary structure of the grating. We perform linear interpolation on the profile line based on the measured data points and the instrument noise level, thereby enhancing the accuracy of boundary recognition. (iii) Calculation of average grating pitch: By utilizing the spatial coordinates of the centroids of each grating structure within the scanning range, we apply a linear fitting method to determine the slope of the fitting line and subsequently compute the average grating pitch.

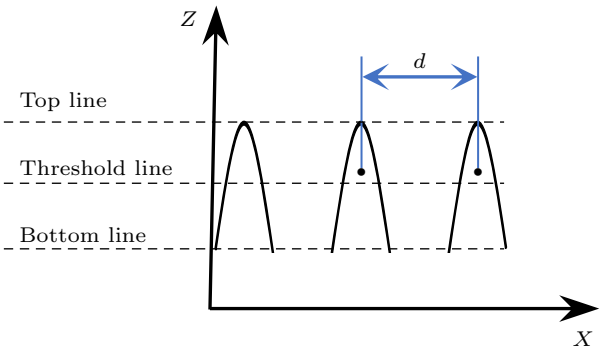


Fig. 4. Principle of the centroid method for calculating grating period.

3. Experiments

This experiment utilizes self-traceable national primary standard materials. The PTB measured the average pitch difference between any two self-traceable gratings, yielding a result of 0.001 nm with an uncertainty of 0.008 nm. The calibrated instrument is a commercial AFM placed in a temperature-controlled room with an ambient temperature of (20 ± 1) °C, temperature fluctuations of ≤ 0.2 °C/h, humidity of $40 \pm 20\%$ RH, and humidity fluctuations of $\leq 5\%$ RH. Prior to calibration, the AFM stage is kept level, and the self-traceable grating sample is allowed to rest on the stage for 30 minutes. When selecting the calibration position, care is taken to avoid areas with pits, scratches, or contamination on the grating.

3.1. AFM calibration method based on self-traceable gratings

In small-scale scanning ranges, measurement errors arise from issues such as the nonlinear effects of the AFM scanning probe and the probe expansion effects, creating an urgent need for calibration. The self-traceable grating exhibits extremely high precision in pitch, exceptional consistency between samples, and well-defined line edges, thereby meeting the nonlinear calibration requirements for AFM in small-scale scans. We employed a one-dimensional Cr self-traceable grating to calibrate the nonlinear errors of the commercial AFM. The images obtained from scanning a 1 μm × 1 μm area of the self-traceable grating are illustrated in Fig. 5.

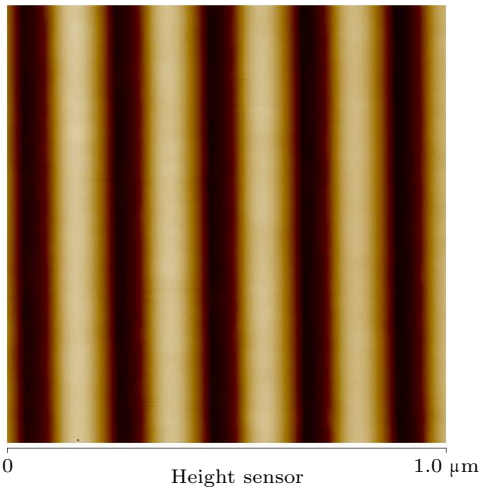


Fig. 5. Image of the self-traceable grating obtained by AFM within a scanning range of 1 μm × 1 μm.

Based on the gravity center method, five positions are randomly selected from each of the four scanned images, and the average period value for each image is calculated, as shown in Table 1. This value was then compared with the average period obtained from the uncalibrated AFM within the same scanning range to derive the calibration factor K, as expressed by the following formula:

$$K = \frac{d_{\mathrm{Cr}}}{d_{\mathrm{AFM}}}$$

where d_{Cr} is the period of the self-traceable grating obtained using the gravity center method, and d_{AFM} is the period measured by the uncalibrated AFM. Given that the pitch of the self-traceable grating is $d = 212.782 \pm 0.008$ nm ($k = 2$), the calibration factor K is determined to be 0.9922.

Table 1. Calibration factor obtained from the comparison of the self-traceable grating period $d = 212.782 \pm 0.008$ nm ($k = 2$) with the uncalibrated AFM.

Number	Area 1	Area 2	Area 3	Area 4	Area 5	Average period (nm)	Calibration factor K
Image 1	214.399	214.425	214.336	214.468	214.373	214.400	0.9925
Image 2	214.429	214.261	214.274	214.533	214.340	214.367	0.9926
Image 3	213.922	214.753	214.686	214.534	214.768	214.533	0.9918
Image 4	214.467	214.461	214.398	214.527	214.483	214.467	0.9921

3.2. Characterization of multilayer film gratings post-calibrated AFM

Following the precise calibration of the AFM, we employed it to measure the period of Si/SiO_2 multilayer film grating samples with a nominal value of 25 nm. Scanning was conducted at ten randomly selected positions across the top, middle, and bottom regions of the sample. To account for the differing nonlinear effects associated with various scanning ranges, we chose a scanning area of 1 μm × 1 μm, which corresponds to the scale of the self-traceable grating used during the AFM calibration, as depicted in Fig. 6.

The acquired grating scanning images were imported into Matlab software, where the gravity center method described in Subsection 2.3 was employed to calculate the period of the multilayer film gratings. To convert these measurements into final AFM results, we multiplied the measured values by the calibration factor K. The calculated measurement values for the period of the multilayer film gratings are presented in Table 2. Based on the calibration using self-traceable gratings, the final linewidth value determined by the AFM is 24.40 nm, with a standard deviation of 0.11 nm.

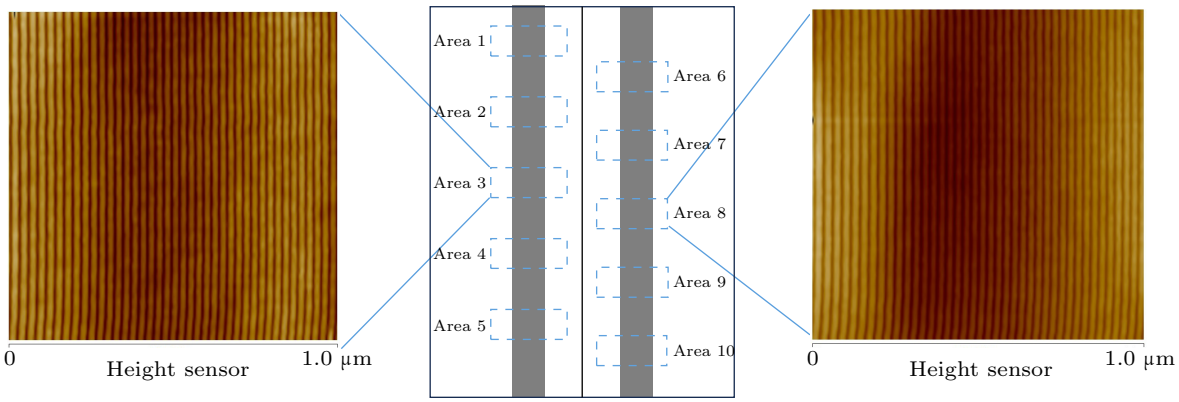


Fig. 6. Image of the multilayer film grating structure obtained by AFM within a scanning range of 1 μm × 1 μm.

Table 2. Calibrated results of multilayer film gratings before and after AFM calibration.

Number	Original period (nm)	Calibrated period (nm)	Number	Original period (nm)	Calibrated period (nm)
1	24.51	24.32	6	24.39	24.20
2	24.65	24.46	7	24.74	24.55
3	24.69	24.50	8	24.57	24.38
4	24.57	24.38	9	24.72	24.53
5	24.48	24.30	10	24.59	24.40
Average period (nm)		24.40	Standard deviation (nm)		0.11

3.3. TEM validation measurements based on Si lattice

To cross-validate the integrity of the self-traceable system and the feasibility of calibration, a Si lattice-calibrated TEM was employed as the verification method. The measurements were performed using a Talos F200X G2 transmission electron microscope. Given that the multilayer film samples were composed of amorphous Si and lacked information on Si crystal planes necessary for direct measurement, it was essential to extract Si crystal plane information from the underlying Si substrate. For traceable measurements, the structure of the multilayer film Si grating and the Si substrate was displayed at a magnification of 36k, with localized measurements conducted at a magnification of 500k, as illustrated in Fig. 7(a). In the high-magnification TEM measurement mode, accurate Si lattice periods were derived from the interference pattern of the transmitted electron beam, yielding TEM images that are traceable to SI units. This approach utilizes the Si lattice spacing as a reproducible method for defining the meter at the nanoscale. Figure 7(b) illustrates the structure of the multilayer film grating at a magnification of 22.5k.

The specific calibration procedure is as follows. The micrograph of the Si lattice spacing obtained from the TEM at a magnification of 500k was analyzed using the integrated software Digital Micrograph. Ten lattice spacings were selected from the scanned image, as shown in Fig. 8. A total of ten measurements were repeated to determine the calibration fac-

tor for the Si lattice-calibrated TEM:

$$k = \frac{d_{10}}{px_{10}} \cdot \frac{px_{\mathrm{Si}}}{T_{\mathrm{Si}}} \cdot \frac{1}{d_{\mathrm{Si}}},$$

where d_{10} is the 10 nm calibration standard, px_{10} is the number of pixels corresponding to the 10 nm standard, px_{Si} is the number of pixels corresponding to the lattice periods of Si lattice T_{Si}, and d_{Si} is the lattice length of Si in the $\langle 111 \rangle$ crystallographic direction, with $d_{\mathrm{Si}} = 0.314$ nm. Thus, the calibration factor $k = 0.987$.

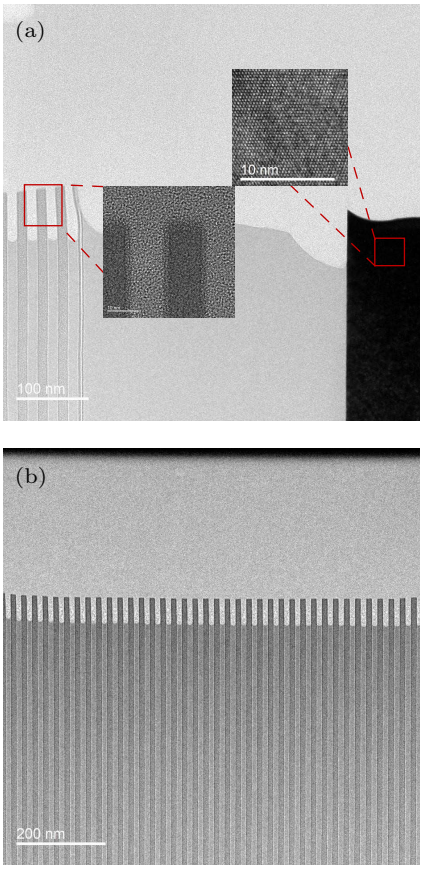


Fig. 7. (a) TEM image of the multilayer film grating structure and Si substrate; (b) TEM image of the multilayer film grating structure.

Table 3. Calibrated results of multilayer film gratings before and after TEM calibration.

Number	Original period (nm)	Calibrated period (nm)	Number	Original period (nm)	Calibrated period (nm)
1	24.55	24.23	6	24.81	24.49
2	24.72	24.40	7	24.86	24.54
3	24.47	24.15	8	24.81	24.49
4	24.59	24.27	9	24.73	24.41
5	24.51	24.19	10	24.59	24.27
Average period (nm)		24.34	Standard deviation (nm)		0.14

At the same scale (10 nm), we conducted multiple scans of the multilayer structure using TEM. Figure 8(b) presents a single multilayer structure at a magnification of 500k, with the image imported into Matlab for analysis. By measuring the number of pixel points corresponding to the period of the single multilayer film and applying the previously calculated calibration factor, we obtained the final calibrated result for the multilayer film based on the Si lattice calibration as 24.34 nm, with a standard deviation of 0.14 nm. The specific measurement results are detailed in Table 3.

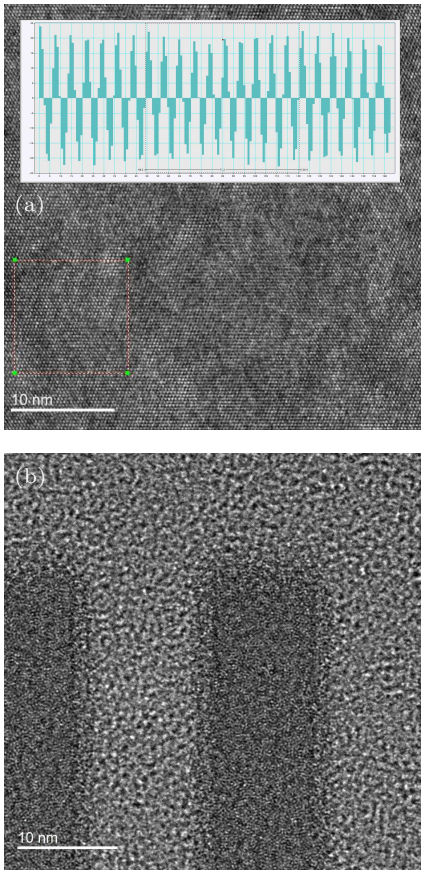


Fig. 8. (a) Pixel points of the Si $\langle 111 \rangle$ crystal plane spacing. (b) Pitch of a single period of the multilayer film.

3.4. Discussion

We employed the AFM calibrated using the self-traceable grating to ascertain the period of the multilayer film grating and conducted a comparative analysis with the results obtained from TEM calibrated against the Si lattice constant. Our results reveal a measurement value deviation of 0.06 nm between the two calibration methods, corresponding to a relative error of 0.25%. This consistency between the measurement outcomes substantiates the coherence of value transfer within both the self-traceable grating traceability chain and the Si lattice traceability chain.

4. Conclusion and perspectives

In the realm of nano-manufacturing, precision measurement technology is pivotal for ensuring product quality and performance. Achieving high accuracy and reliability necessitates consistency across various measurement systems. This study introduces a novel shortened traceability chain based on the Cr atomic transition frequency ($^7S_3 \rightarrow {}^7P_4$) and utilizes self-traceable gratings fabricated via atomic lithography

to calibrate AFM nonlinearities and probe expansion effects, specifically for determining the period of a Si/SiO_2 multilayer film grating with a nominal value of 25 nm. Validation results show a measured value of 24.40 nm using the self-traceable grating calibration system, closely aligning with the TEM result of 24.34 nm calibrated against the Si lattice constant. This agreement confirms the accuracy of the self-traceable shortened traceability system.

In this static calibration process, the method not only enhances calibration convenience but also enables direct calibration in real working environments, effectively avoiding potential errors from equipment relocation. Additionally, this approach offers nondestructive measurement, crucial for preserving high-value, fragile, or irreplaceable samples. It allows precise measurement without compromising sample integrity, thus ensuring the authenticity of measurement data. Furthermore, self-traceable gratings can be applied in dynamic calibration by integrating them into grating interferometers, enhancing measurement capability in the micro-displacement domain.[21] However, current limitations in preparation methods and principles restrict the grating area, posing certain constraints. To meet the need for larger measurement areas, the research team is exploring splicing atom lithography[22] to further expand the measurement range.

Acknowledgments

Project supported by the National Natural Science Foundation of China (Grant Nos. 61925504 and 52475563), the National Key Research and Development Program of China (Grant Nos. 2022YFF0607600 and 2022YFF0605502), Key Laboratory of Metrology and Calibration Technology Fund Project (Grant No. JLKG2023001B001), and Aeronautical Science Foundation Project (Grant No. 20230056038001).

References

[1] Dai G, Heidelmann M, Kübel C, Prang R, Flügge J and Bosse H 2013 *Measurement Science and Technology* **24** 085001

[2] Orji N G, Badaroglu M, Barnes B M, Beitia C, Bunday B D, Celano U, Kline R J, Neisser M, Obeng Y and Vladar A E 2018 *Nat. Electron.* **1** 532

[3] Deng X, Yin Z, Dai G, Xiao G, Tang Z, Shen J, Zhou T, Xue D, Xie Y and He C 2024 *Measurement Science and Technology* **35** 125009

[4] Basile G, Bergamin A, Cavagnero G, Mana G, Vittone E and Zosi G 1994 *Phys. Rev. Lett.* **72** 3133

[5] Dai G, Hu X and Degenhardt J 2022 *Surface Topography: Metrology and Properties* **10** 015018

[6] Dirscherl K, Garnæs J, Nielsen L, Jørgensen J F and Sørensen M P 2000 *Journal of Vacuum Science & Technology B: Microelectronics and Nanometer Structures Processing, Measurement and Phenomena* **18** 621

[7] Wu Z, Cai Y, Wang X, Zhang L, Deng X, Cheng X and Li T 2019 *Chin. Phys. B* **28** 030601

[8] McClelland J J, Scholten R E, Palm E C and Celotta R J 1993 *Science* **262** 877

[9] McClelland J J, Anderson W R, Bradley C C, Walkiewicz M, Celotta R J, Jurdik E and Deslattes R D 2003 *Journal of Research of the National Institute of Standards and Technology* **108** 99

[10] Misumi I, Lu M, Tanaka H, Sugawara K, Gonda S and Kurosawa T 2008 *Measurement Science and Technology* **19** 045101

[11] Dai G, Koenders L, Pohlenz F, Dziomba T and Danzebrink H U 2005 *Measurement Science and Technology* **16** 1241

[12] Chen J, Liu J, Wang X, Zhang L, Deng X, Cheng X and Li T 2017 *Measurement Science Review* **17** 264

[13] Dahlen G, Osborn M, Okulan N, Foreman W, Chand A and Foucher J 2005 *Journal of Vacuum Science & Technology B: Microelectronics and Nanometer Structures Processing, Measurement and Phenomena* **23** 2297

[14] Binnig G, Quate C F and Gerber C 1986 *Phys. Rev. Lett.* **56** 930

[15] Dai G, Hahm K, Bosse H and Dixson R G 2017 *Measurement Science and Technology* **28** 065010

[16] Deng X, Li T and Cheng X 2022 *Optics and Precision Engineering* **30** 2608

[17] Kuchibhatla S VNT, Karakoti A S, Bera D and Seal S 2007 *Progress in Materials Science* **52** 699

[18] Misumi I, Dai G, Lu M, Sato O, Sugawara K, Gonda S, Takatsuji T, Danzebrink H U and Koenders L 2010 *Measurement Science and Technology* **21** 035105

[19] Takenaka H, Hatayama M, Ito H, Ohchi T, Takano A, Kurosawa S, Itoh H and Ichimura S 2011 *Journal of Surface Analysis* **17** 264

[20] Misumi I, Gonda S, Kurosawa T and Takamasu K 2003 *Measurement Science and Technology* **14** 463

[21] Lin Z, Yao Y, Zhou T, Xue D, Gu Z, Deng X, Cheng X and Li T 2022 *Metrology Science and Technology* **66** 3

[22] Deng X, Tan W, Tang Z, Lin Z, Cheng X and Li T 2022 *Nanomanufacturing and Metrology* **5** 179